D. ARABELOS
Department of Geodesy and Surveying
University of Thessaloniki
GR-540 06 Thessaloniki (Greece)

C.C. TSCHERNING
Geophysical Institute
University of Copenhagen
Haraldsgade 6 DK-2200 Copenhagen N (Denmark)

SIMULATION OF REGIONAL GRAVITY FIELD RECOVERY FROM SATELLITE GRAVITY GRADIOMETER DATA USING COLLOCATION AND FFT

Abstract

When planning a satellite gravity gradiometer (SGG) mission, it is important to know the quality of the quantities to be recovered at ground level as a function of e.g. satellite altitude, data type and sampling rate, and signal variance and noise. This kind of knowledge may be provided either using the formal error estimates of wanted quantities using least-squares collocation (LSC) or by comparing simulated data at ground level with results computed by methods like LSC or Fast Fourier Transform (FFT).

Results of a regional gravity field recovery in a 10° x 20° *area surrounding the Alps using LSC and FFT are reported. Data used as observations in satellite altitude* (202 *or* 161 km) *and for comparison at ground level were generated using the* OSU86F *coefficient set, complete to degree* 360. *These observations are referred to points across simulated orbits. The simulated quantities were computed for a* 45 *days mission period and* 4 s *sampling. A covariance function which also included terms above degree* 360 *was used for prediction and error estimation. This had the effect that the formal error standard deviations for gravity anomalies were considerably larger than the standard deviations of predicted minus simulated quantities. This shows the importance of using data with frequency content above degree* 360 *in simulation studies. Using data at* 202 km *altitude the standard deviation of the predicted minus simulated data was equal to* 8.3 mgal *for gravity and* 0.33 m *for geoid heights.*

1. Introduction

When planning a satellite gravity gradiometer (SGG) mission, it is important to know the quality (error) of the quantities to be recovered at ground level as a function of e.g. satellite altitude, data type, sampling rate, and signal and noise statistics. This information may be provided either using the formal error estimates of the wanted quantities using least squares collocation (LSC) or by comparing simulated data at ground level with results computed by available methods like LSC, integral formula methods or (fast) Fourier techniques (FFT). We will here only consider the regional recovery, primarily because the methods we want to discuss (with the present computers) are difficult to use for the global recovery. Here other methods are available, see e.g. Colombo (1984), Vermeer (1989).

A survey of available methods for regional gravity field recovery from SGG data is given in Tscherning et al. (1989). In between the there discussed methods, LSC is the most general tool because it both permits the estimation of the error of computed (= "predicted") quantities as well as the comparison of predicted data with simulated ground data. The method, however, is computationally costly, because a (full) system of equations has to be solved with as many unknowns as the number of SGG observations used.

If gridded data are available (e.g. provided by using LSC locally), then fast methods like FFT can be used.

The LSC and the FFT methods have both been implemented as FORTRAN-program modules within the GRAVSOFT package, developed at Kort- og Matrikelstyrelsen (National Survey and Cadastre, Denmark) and at Geophysical Institute, University of Copenhagen. The package has been extended and upgraded in order to provide a general tool for the study of the quality of regional gravity field recovery from SGG data, and hopefully in the not too distant future for the actual recovery using real data. In this report we will describe results in a $10° \times 20°$ area surrounding the Alps, using LSC and FFT. We present here a general scheme, which can be used for the study of the influence of mission and instrument parameters as well as the dependence of the results due to the change in statistical gravity field characteristics from region to region.

Obviously the methods are so general that they may be used to study other types of gravity field survey projects (Tscherning, 1975, 1980, 1983), but this will not be discussed here. Earlier studies using SGG data and collocation regionally are reported e.g. in Robbins (1985), Tscherning (1987, 1988), where also further references may be found.

2. Generation of data point configurations of SGG data and of data to be used for comparison

A satellite gravity gradiometer is expected to fly in an altitude between 160 km to 250 km. At these altitudes the orbit will depend strongly on the spherical harmonic coefficients up to a high degree and order. Orbit calculations have been executed using a coefficient set up to degree 360. However, for the purpose of studying gravity field recovery, the orbits need not to be known very accurately. On the other hand, the real orbits will not be located at a surface with a constant altitude above the Earth ellipsoid. We therefore decided to use orbits generated by a gravity field which included the central term and the C_{20} term, which determines the main perturbations of a pure Keplerian orbit. A computer program (received from E. Schrama, Delft) was modified as to provide (geodetic) coordinates of a satellite with given initial semimajor axis (a), eccentricity and inclination at given time intervals. Depending on a "mode" parameter, it will also provide the components of the satellite velocity vector, which may be used if data are to be referenced to an orbit or instrument dependent frame (otherwise the traditional East, North and (radially) Up frame is used).

The program was used to generate fictitious observation points at various altitudes in a $10° \times 20°$ test area, surrounding the Alps, see *Figure 1.* The initial value

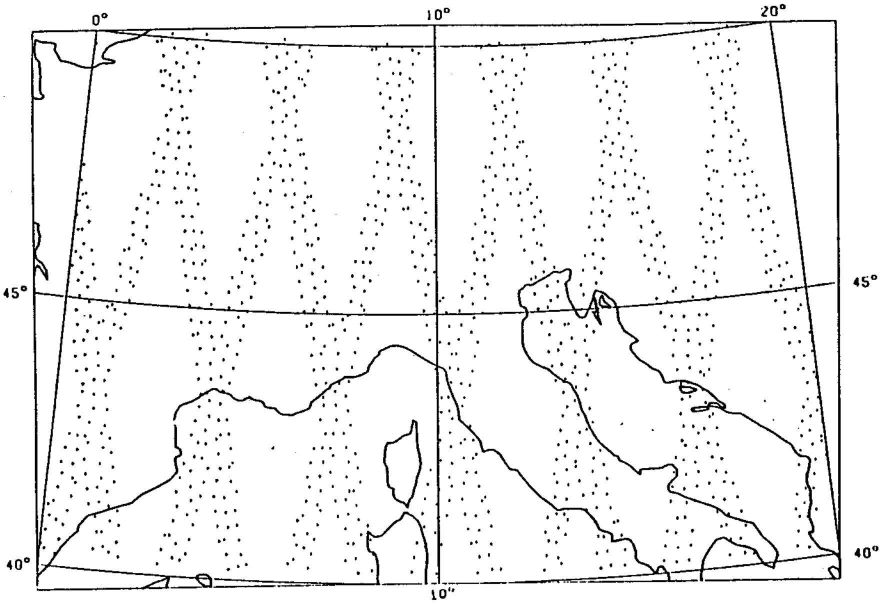

Fig. 1 – Distribution of simulated T_{zz} *observations used in the first experiment with* $h = 200$ km .

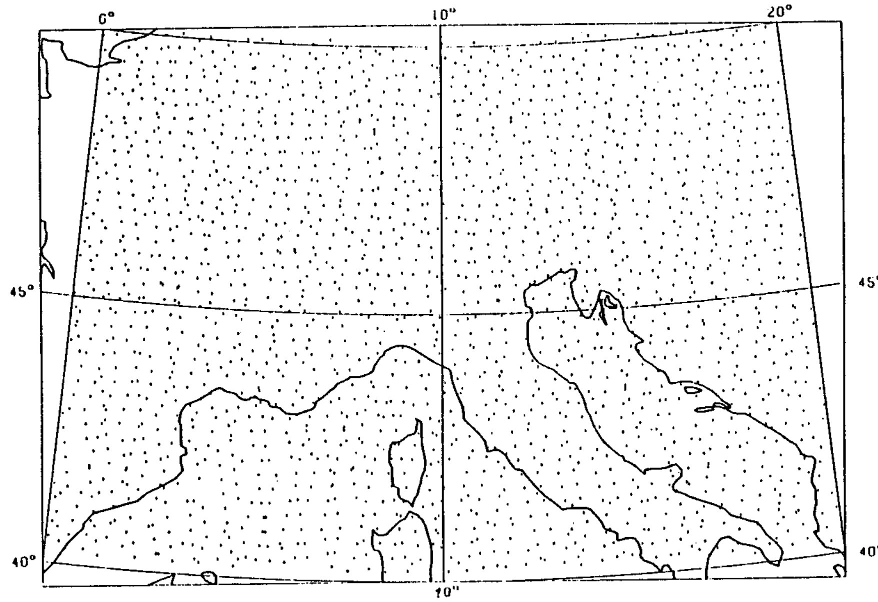

Fig. 2 – Distribution of simulated T_{zz} *observations used with* $h = 202$ km.

of the satellite orbit axis must be selected with care, in order to obtain a homogeneous data distribution during a mission duration of a few months. In ***Figure 1*** the subsatellite points are shown for a height $h = 200$ km for a 45 days mission duration and 4 s sampling. ***Figure 2*** shows the distribution for $h = 202$ km, after a selection of one point in each $15' \times 20'$ cell has been made. (This selection eliminated about 50 % of the points and has already been applied to the data in ***Figure 1***).

Noise-free SGG data may then be generated using a spherical harmonic expansion. For this purpose, we used the OSU86F coefficient set (Rapp and Cruz, 1986), and calculated the various SGG quantities using the subroutine GPOTDR (Tscherning et al., 1983) which forms a part of the GEOCOL program (Tscherning 1974, 1989).

The OSU86F set is complete to degree and order 360. Using this we naturally eliminate the influence of higher order frequencies. However, if we study the recovery of e.g. $1° \times 1°$ mean gravity or geoid heights at the Earth's surface, then these frequencies are not very important. For smaller blocks, we should then generate SGG data using local information (e.g. $10' \times 20'$ mean gravity data). This is also possible using GEOCOL, but was not used here due to computer time limitations. (It is rather time consuming).

Using GEOCOL, files with the following gravity gradients were generated :

$$T_{zz} = \frac{\partial^2 T}{\partial z^2}, \; T_{zx} = \frac{\partial^2 T}{\partial z \, \partial x}, \; T_{zy} = \frac{\partial^2 T}{\partial z \, \partial y}, \; 2T_{xy} = 2\frac{\partial^2 T}{\partial x \, \partial y}, \; T_{\Delta} = \frac{\partial^2 T}{\partial y^2} - \frac{\partial^2 T}{\partial x^2}$$

As discussed in Tscherning et al. (1989) it is advantageous to subtract the effect of a known spherical harmonic expansion. We here decided to subtract the effect of GPM2 (Wenzel, 1985) to degree 60. This coefficient set has low degree coefficients different from those of the OSU86F set. We should then be able to see the error due to the errors in the low order harmonics. In ***Figures 3*** and ***4*** we see the free-air gravity anomalies and the geoid heights at 5 km altitude generated by the OSU86F–GPM2 (to degree 60) coefficients. The altitude 5 km was selected in order to obtain quantities with spectral content similar to $0°.5 \times 0°.5$ anomalies. In ***Figures 5*** and ***6*** we see T_{zz} at 202 and 161 km altitude. Note the very strong signal over the Alps, and the much larger values of T_{zz} at 161 km as compared to values at 202 km.

The simulated quantities were computed for a 45 day period. For the $10° \times 20°$ area this resulted in more than 3000 points, which with 5 independent quantities per point maximally give 15000 simulated data. A full system with so many unknowns is too large for present day minicomputers. But as we shall see later, it is not necessary to deal with all simulated observations simultaneously. However, we would like to make simulations with at least 2 components simultaneously, covering the whole area. Here a reasonable total number of data is about 2×1600. We therefore made a selection of the data points, so that one simulated observation per $15' \times 20'$ cell was selected.

Simultaneously with the data selection, normal distributed random noise with given standard deviation was added. Here we use the algorithm described in Press et al. (1986) for the generation of the noise. Optionally, a systematic bias could be added to each track. The bias would for each track have a random distribution with given standard deviation.

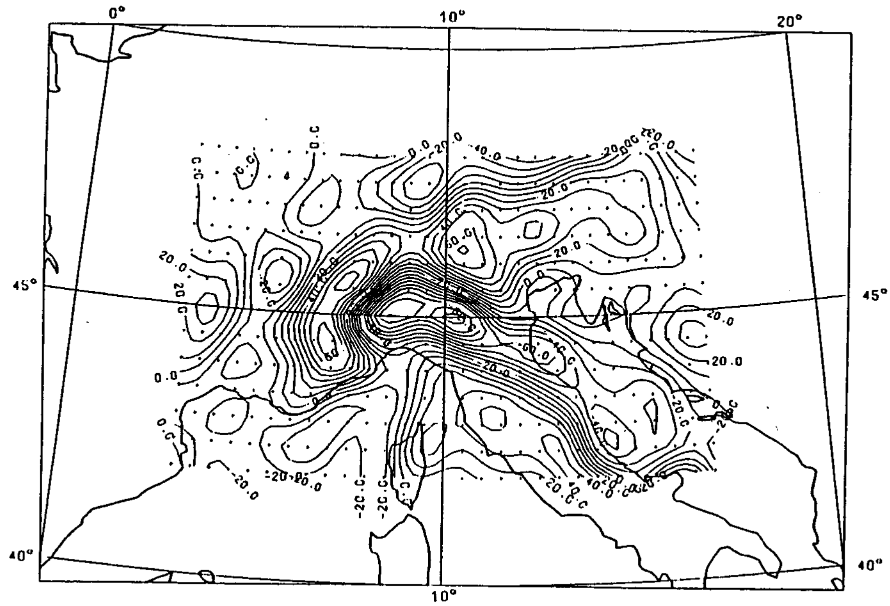

Fig. 3 – Free-air gravity anomalies (mgal) *at* 5 km *altitude produced by subtracting the contribution from* GPM2 *to degree* 60. *Contour interval* 10 mgal.

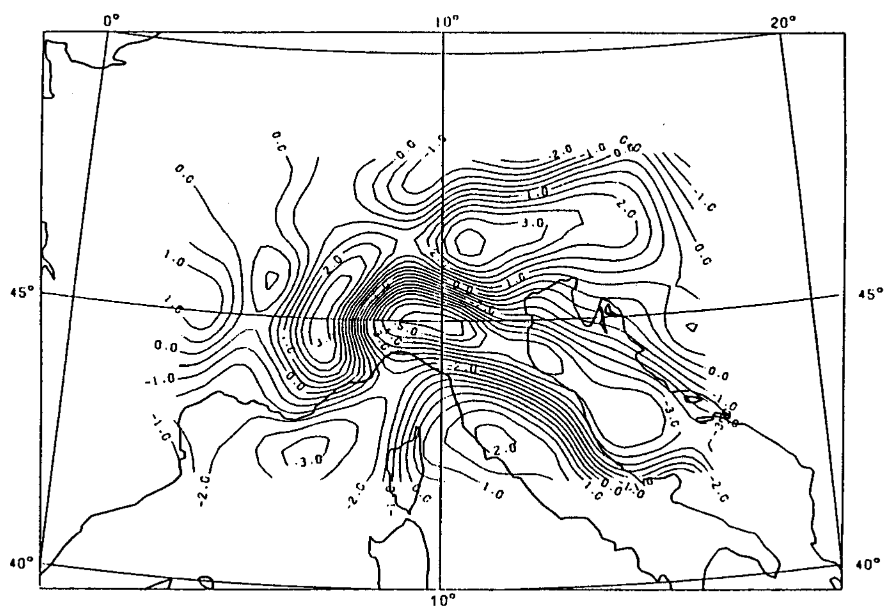

Fig. 4 – Geoid height (m) *at* 5 km *altitude produced by the* OSU86F *coefficients minus the contribution from* GPM2 *to degree* 60. *Contour interval* 0.5 m.

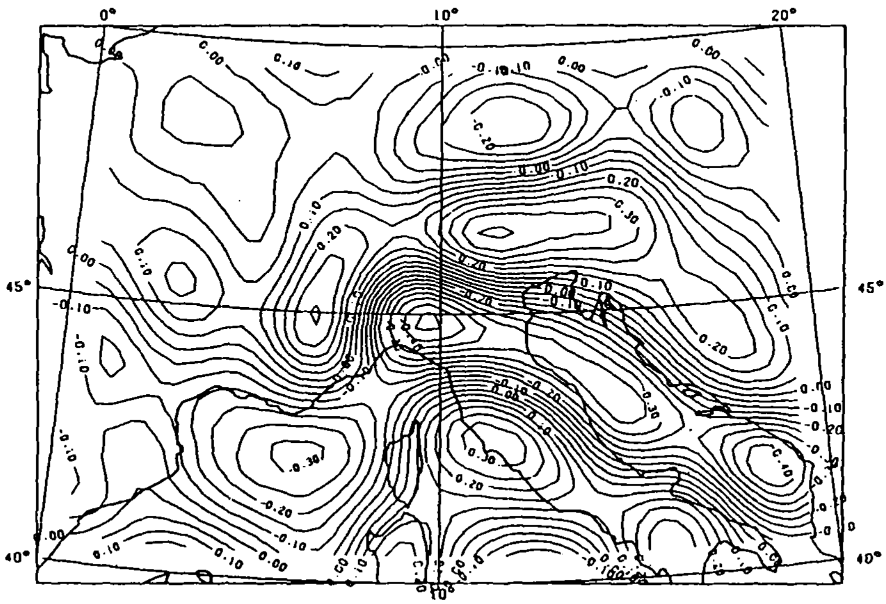

Fig. 5 – T_{zz} *at* 200 km *altitude predicted from* T_{zz} *generated with* h = 202 km *(cf. Fig. 2). Based on the* OSU86F *coefficients minus the contribution from* GPM2 *to degree* 60. *Contour interval* 0.05 E.U.

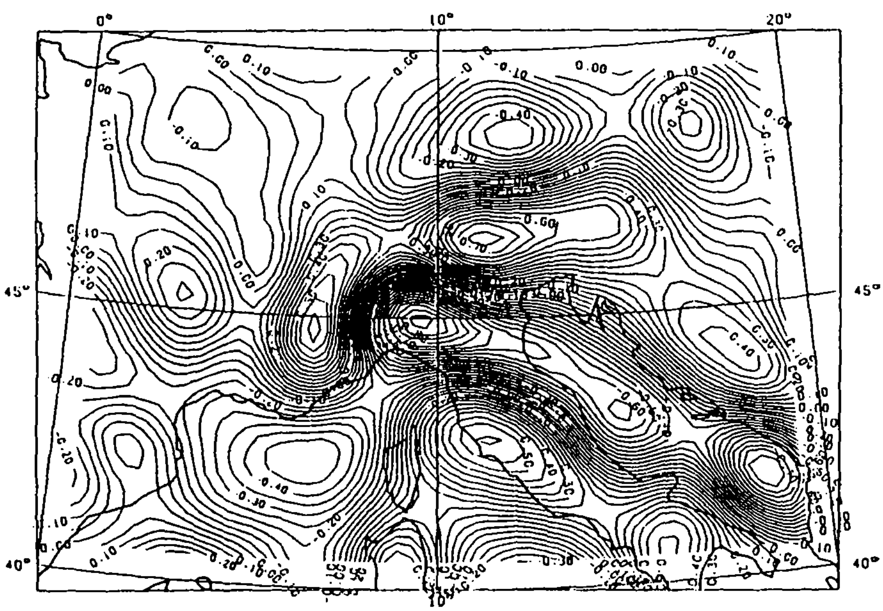

Fig. 6 – T_{zz} *at* 161 km*, generated like in Fig. 5. Contour interval* 0.05 E.U. *Note the much stronger signal.*

Three new files were generated per data type, with 0.01, 0.02 and 0.03 E.U. noise standard deviations added. Files with track bias with standard deviations of 0.01 and 0.1 E.U. were also created for simulated observations of type T_{zz} .

3. Selection of covariance function model

The residual observation files may be used to compute a so-called empirical covariance function. Covariances are computed by forming mean values of products of gradients, sampled with respect to the spherical distance between the observation points. In theory, the points must be in the same altitude. The empirical values for T_{zz} at 202 km altitude are shown in *Figure 7.*

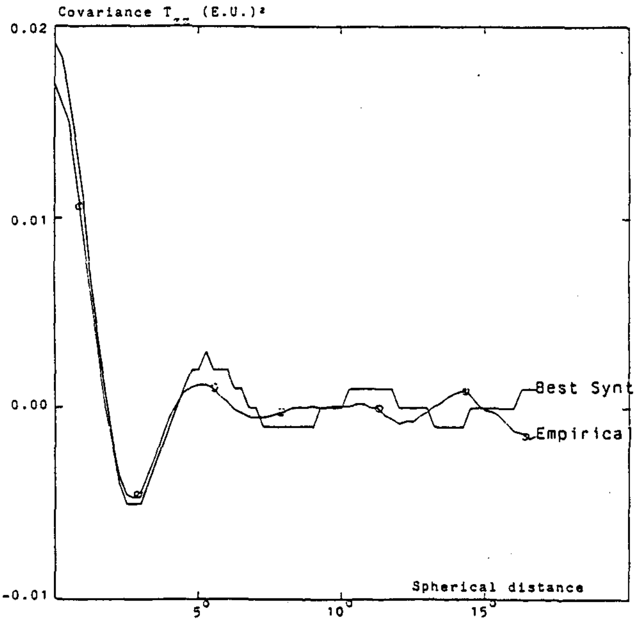

Fig. 7 — Empirical and best fitting synthetic covariance function of T_{zz} *generated at* h = 202 km. *Synthetic covariance function generated using depth to Bjerhammar sphere* 564 m, *gravity variance at ground level* 1142 mgal^2 *and scale factor on error degree variances* 0.05 .

These values may be represented using an analytical expression, see Knudsen, (1987), Tscherning et al. (1989). However, this resulted in a covariance function with too small gravity anomaly variance at the Earth's surface (600 mgal^2) , where we would expect a much higher value for the area of the Alps. This is naturally an effect of not using simulated observations which include information from coefficients above degree 360 . The analytic expression (see *Figure 7*), also had a radius of the Bjerhammar-sphere closer to the mean radius of the Earth, (100 – 500 m difference) than normally found in practice.

We therefore decided to select a function, based on our experience with data from a similar area. We forced the covariance function to have a gravity anomaly variance of $1400\ \mathrm{mgal}^2$, and a depth to the Bjerhammar-sphere of $1.7\ \mathrm{km}$. The resulting covariance function of T_{zz} is shown in ***Figure 8.*** Most important is, that it has a variance 50 % larger than the one determined empirically. We thus have a covariance function which is inconsistent with the simulated data used, but probably much more realistically modelling the true gravity field.

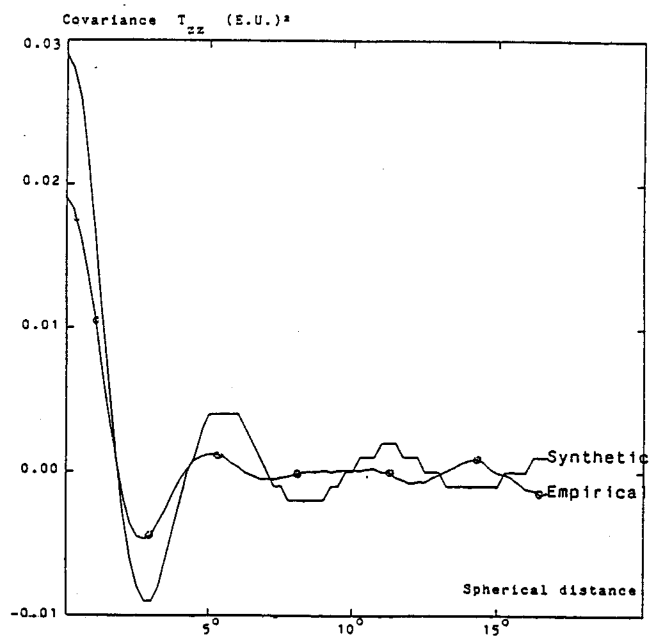

Fig. 8 — Empirical and synthetic covariance function of T_{zz} *at* $h = 202\ \mathrm{km}$. ***The synthetic covariance function was used in the predictions. Depth to Bjerhammar sphere*** $1700\ \mathrm{m}$, ***gravity variance at ground level*** $1400\ \mathrm{mgal}^2$ ***and scale factor on error degree variances*** 0.05.

The initial analysis was done using T_{zz} data only. However, empirical covariance functions were computed using the pairs (T_{xz}, T_{yz}) and $(2T_{xy}, T_{\Delta})$ also. They were then compared with the analytically derived functions, and a good agreement was found. As a final test of the consistency of the analytic model, one kind of gravity gradient was used to compute the other. Also here an excellent agreement was found.

4. Computation of error estimates and comparison of simulated observed and predicted values

We first used the test data generated at $h = 200\ \mathrm{km}$ *(Fig. 1)*, without observing that it contained large gaps between the data. Using the T_{zz} component, gravity and geoid heights were predicted at $5\ \mathrm{km}$ altitude, and compared with the "ground truth values". The results showed large unexpected errors (30 mgal) in areas where the gravity field was rather smooth (compared to the Alps) even using noise free data. When we plotted the error estimates we also saw the influence of the data distribution. This gave us a useful information, so subsequently we used mean orbit heights to $h = 202660$ m and 161523 m, and in each case an inclination of 96°.4 and eccentricity $c = 0.0051$.

The quality of a gravity field recovery is generally expressed in terms of the error in mean gravity anomaly or geoid heights of a certain block-size, e.g. 0°.5 x 0°.5 or 1° x 1°. Such mean values will have to be evaluated by numerical integration of point values, predicted typically in a 5 x 5 set of points within the block. However, the smoothing performed during the formation of a mean value corresponds closely to an upward continuation, see Tscherning and Rapp (1974). For 0°.5 x 0°.5 the corresponding height is approximately 5 km. We therefore decided to compare results obtained using point values at 5 km height with values obtained from numerical integration of values in a 5 x 5 set of points.

Table 1

Differences between 377 observed and computed 0°.5 x 0°.5 mean gravity anomalies and point values at 5 km height using T_{zz}-data at 202 km altitude. Values from an area

$42° \leq \varphi \leq 48°$, $3° \leq \lambda \leq 17°$

		observed mgal	predicted mgal	difference mgal
Results based on data at 5 km height	mean	– 0.3	– 0.4	0.0
	std.dev.	29.4	27.6	9.5
0°.5 x 0°.5 mean values	mean	– 0.2	– 0.4	0.1
	std.dev.	30.9	29.2	10.2

Table 1 shows that the statistical results using point values at 5 km altitude are nearly identical to those obtained using half degree mean values. Since the 5 km values are much more easy to obtain (1/25 computational effort), we decided to use these values in the subsequent computations.

Systematic simulations were then executed using various gradient components, either individually or in pairs : T_{zz}, T_{zx} T_{zy}, $2T_{xy}$. T_{Δ}, (T_{zx}, T_{zy}) . and $(2Txy, T_{\Delta})$ with noise level 0.01, 0.02 and 0.03 E.U. In each case 377 point values were computed at points spaced 0°.5 apart at 5 km altitude, and compared with test values. *Table 2* and *2a* give results of comparisons using $h = 202$ and 162 km, respectively. Results obtained using T_{zz} only are shown in ***Figures 9–12.*** Note that a border zone of 2° is excluded.

Also the result of the error estimate of one point in the middle of the area is given. Note, that this estimate for gravity values is much larger than the one obtained by comparing simulated observed and computed quantities. This is due to the fact, that especially the gravity anomaly covariance function contains frequencies which are significant above degree 360, while the test data do not. The error estimate may be

Table 2

Results of prediction, at 202 km height

n = number of points. σ_c = standard error from collocation. $\bar{x}$ = mean of difference. σ = standard deviation of differences.

Noise level (E.U.)	Input data type	n =	T_{zz} 1869	T_{zx}, T_{zy} 3024	$2\,T_{xy}, T_{\Delta}$ 3024	T_{zx} 1869	T_{zy} 1869	$2\,T_{xy}$ 1869	T_{Δ} 1869
0.01	Δg (mgal)	$\bar{x}$	−0.18	−0.68	0.24	−2.36	−1.20	−1.79	−0.21
		σ	8.31	9.46	9.43	13.89	12.89	20.79	13.37
		σ_c	17.05	16.96	16.81				
	ζ (m)	$\bar{x}$	−0.42	−0.44	−0.33	−0.60	−0.49	−0.55	−0.43
		σ	0.33	0.32	0.38	0.78	0.92	1.94	0.98
		σ_c	0.32	0.32	0.31				
0.02	Δg (mgal)	$\bar{x}$	−0.18	−0.74	−0.97				
		σ	8.92	10.16	10.39				
		σ_c	17.92	17.86	17.67				
	ζ (m)	$\bar{x}$	−0.43	−0.45	−0.41				
		σ	0.35	0.37	0.41				
		σ_c	0.37	0.36	0.35				
0.03	Δg (mgal)	$\bar{x}$	−0.28	−0.59	−1.08				
		σ	9.81	10.70	11.29				
		σ_c	18.50	18.41	18.23				
	ζ (m)	$\bar{x}$	−0.43	−0.44	−0.44				
		σ	0.39	0.43	0.44				
		σ_c	0.40	0.40	0.39				

Table 2a

Prediction results for $0°.5$ mean values (377 points at 5 km height) from data at 161.523 km height. The level of the noise of the data is 0.01 E.U. ; n = number of input points used.
$\bar{x}$ = mean value, σ = standard deviation.

			input data type	T_{zz}	T_{zx} , T_{zy}	$2T_{xy}$, T_{Δ}
			n	1875	2714	2714
		obs.		obs.-pred.		
Δg (mgal)	$\bar{x}$	−0.35		−0.46	−0.47	0.51
	σ	29.37		5.86	5.97	6.54
ζ (m)	$\bar{x}$	0.42		−0.42	−0.44	−0.32
	σ	1.91		0.30	0.21	0.32

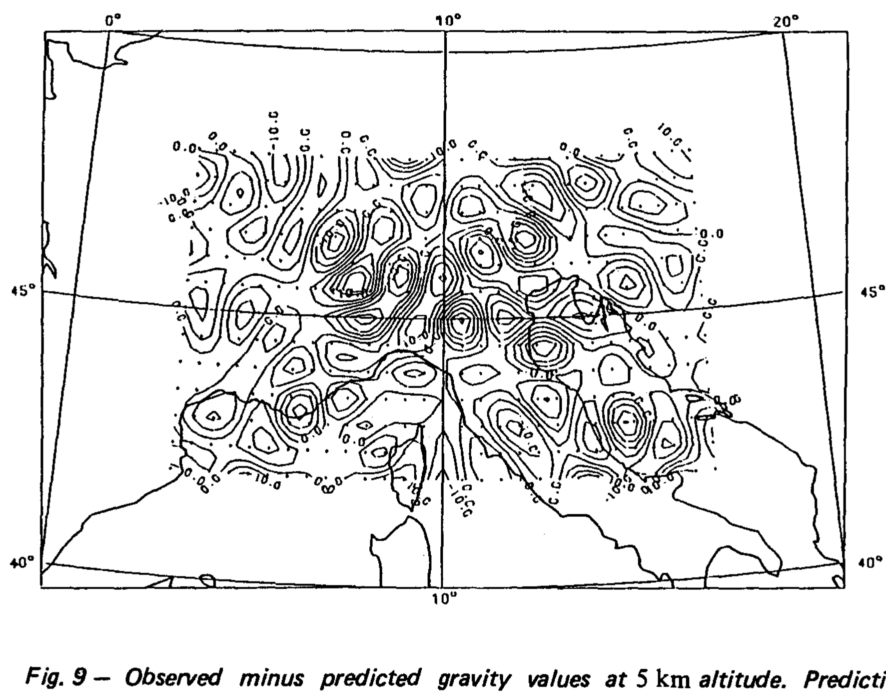

Fig. 9 – Observed minus predicted gravity values at 5 km altitude. Prediction based on T_{zz} values at 202 km altitude with 0.01 E.U.; random noise added. Contour interval 5 mgal.

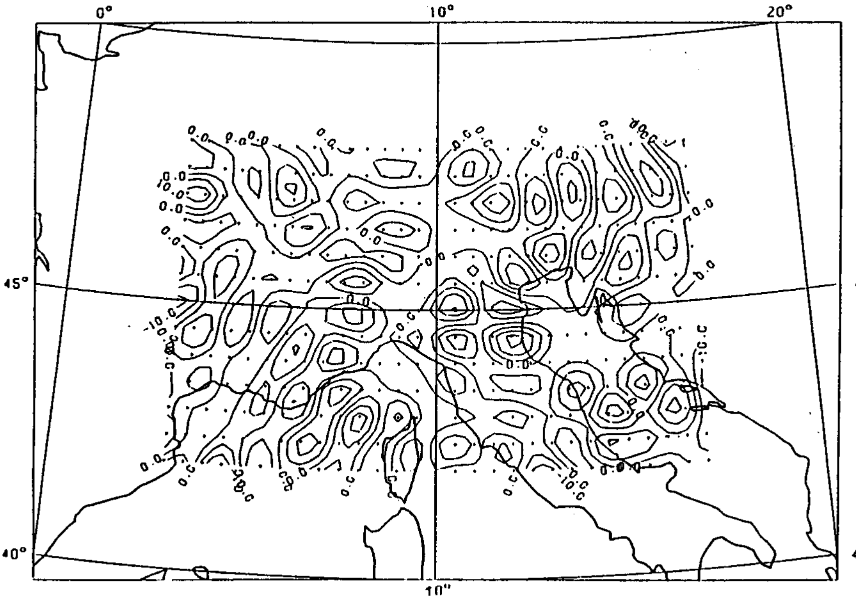

Fig. 10 – Observed minus predicted gravity values at 5 km *altitude. Prediction based on* T_{zz} *values at* 160 km *altitude with* 0.01 E.U.; *random noise added. Contour interval* 5 mgal.

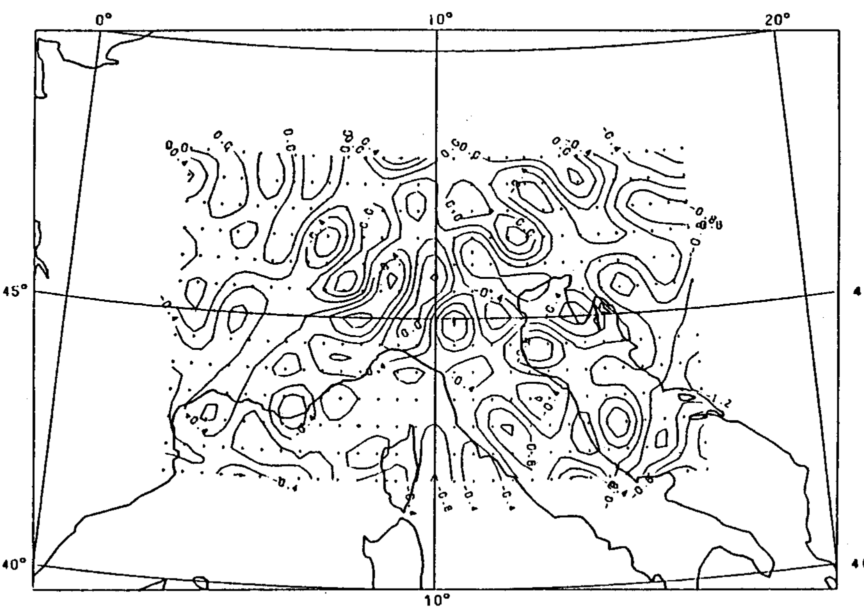

Fig. 11 – Observed minus predicted geoid heights at 5 km *altitude.* T_{zz} *at* 202 km *altitude with* 0.01 E.U.;*random noise added. Contour interval* 0.2 m.

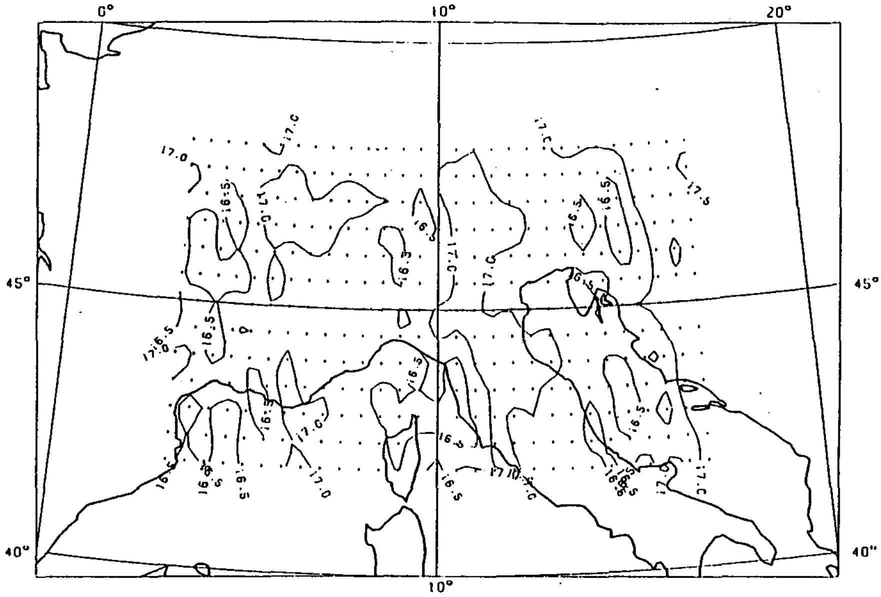

Fig. 12 — Collocation error estimation of predicted gravity values at 5 km *altitude based on* T_{zz} *at* 202 km *altitude. Contour interval* 0.5 mgal .

regarded as realistic, and shows that we should try to eliminate the higher frequencies, e.g. by subtracting topographic effects as discussed in Tscherning et al. (1989). Note that the simulated observations have mean values and standard deviations equal to − 0.3, 29.4 mgal and − 0.42, 1.91 m for gravity anomalies and geoid heights at 5 km altitude, respectively.

From the test data spaced 0°.5 apart, 1° mean values were computed. The result of the comparison is given in *Table 3,* for h = 202 km .

Note that we naturally get the best results using data with the smallest noise added. However, the decrease in the quality of the prediction is not severe, showing the effect of the filtering made using LSC. In all cases the best results are obtained using T_{zz} . Even using two "horizontal" components simultaneously does not give better results, but it gives naturally better results than using only one horizontal component. The reason is here to a high degree, that T_{zz} has a higher signal variance, i.e. the signal to noise ratio becomes the best. Note that in all cases the data used for comparison cover a smaller area than the test observations.

For geoid heights it is also interesting to note the large bias. This shows that we are not able to obtain good absolute geoid heights, but only good height differences. For the determination of absolute geoid heights, a global data coverage is needed or a better low order reference field.

Due to computer cost limitations, it was not possible to use all the data simultaneously. However, local solutions may be computed for sub-areas, and then fitted together. This was done using noise of 0.01 E.U. Each sub-area had an extent

Table 3

Results of prediction of 1° x 1° mean values using data in the 10° x 20° area. Altitude 202660 m.

Derived from results in Table 2 taking mean values of 2 x 2 half-degree blocks.

Noise level (E.U.)				T_{zz}	T_{zx}, T_{zy}	$2T_{xy}, T_\Delta$	T_{zx}	T_{zy}	$2T_{xy}$	T_Δ
			obs	obs–pred						
0.01	Δg (mgal)	$\bar{x}$	−0.15	−0.05	−0.19	0.00	−2.47	−1.43	−2.20	−0.36
		σ	24.45	5.36	6.40	6.21	10.75	9.48	18.28	10.30
	ζ (m)	$\bar{x}$	−0.44	−0.42	−0.42	−0.37	−0.61	−0.54	−0.59	−0.45
		σ	1.72	0.28	0.25	0.34	0.72	0.87	1.86	0.92
0.02	Δg (mgal)	$\bar{x}$		−0.07	−0.72	−1.71				
		σ		6.12	6.84	7.65				
	ζ (m)	$\bar{x}$		−0.43	−0.46	−0.45				
		σ		0.30	0.31	0.38				
0.03	Δg (mgal)	$\bar{x}$		−0.13	−0.76	−1.65				
		σ		6.80	7.29	7.97				
	ζ (m)	$\bar{x}$		−0.44	−0.47	−0.47				
		σ		0.33	0.36	0.38				

of 4°.5 x 6°, and the result in the 1°.5 x 2° inner area was used, i.e. the blocks had an overlap of 1°.5 x 2° (a larger overlap of 3° x 3°.5 did not make any difference).

Table 4 gives the result for all the blocks, using all 5 components. The gravity and geoid mean and standard deviation is given for both the simulated observations and for the difference between observed and predicted values. Note again the very small biases for the predicted gravity values, but the large biases for the geoid heights.

The joint result was that gravity values were predicted with a mean error and standard deviation of 0.1 mgal, and 7.6 mgal, respectively. For geoid heights, the result was −0.39 m and 0.31 m mean and standard deviation, respectively. This result is slightly better than the result obtained using T_{zz} alone, cf. *Table 2.*

The results were compared at the block boundaries, and some differences of the magnitude 2–3 mgal were found. The magnitude of the differences is largest, where we find the largest gravity variations at the block boundaries.

LSC permits that data at the Earth's surface are also included in the solution. We tried to use 4 points with gravity and geoid heights in the middle of the test area. However, no significant improvement was observed.

The influence of systematic instrument errors was also investigated. Random biases were added to T_{zz} data on each orbit, and subsequently recovered using LSC. Biases with standard deviation of 0.01 and 0.1 E.U. were added. The result was nearly identical to the result obtained with no bias, cf. *Table 2.* The gravity error was 8.7 mgal as compared to 8.3 mgal.

We also made several tests trying various combinations of the data. The improvements with respect to using T_{zz} alone were marginal. The reason is, that the field is already well determined using T_{zz}, i.e. the quantities are strongly correlated. As mentioned in section 3, we predicted the different gradients from T_{zz} in order to check the consistency of the covariance function computation procedure. The result of the prediction is given in *Table 5.*

Also the influence of changing the covariance function was tested. Again here the changes were not large as the changes were of a reasonable magnitude (Bjerhammar-sphere radius −0.5 km, point gravity variance of Earth's surface 400 $mgal^2$).

Through the various test computations we have gained new insight into the use of LSC for gravity field recovery from SGG :

(a) The successful recovery in the case of biases and tilts is obvious.

(b) The (small) improvement gained when combining all data, and using small blocks.

(c) The limited influence of increased noise on the result.

(d) The relative contribution of the different gradient components to the result (T_{zz} major contributor).

(e) The too optimistic results obtained using 0°.5 gravity data for comparison, when only a 360 degree field is used for the test data generation. (However, results in terms of geoid recovery are more realistic, except for a large bias).

Test computations were exclusively performed using data given in a geographical reference frame. But results using data in a satellite orbit reference frame should not be different.

Table 4

Results of prediction of $1^\circ.5 \times 2^\circ$ blocks from data in $4^\circ.5 \times 6^\circ$ blocks. n = number of points given in brackets. Boundaries of local solution are indicated.

			3° obs	obs–pred	5° obs	obs–pred	7° obs	obs–pred	9° obs	obs–pred	11° obs	obs–pred	13° obs	obs–pred	15° obs	obs–pred 17°
−48°			n = (1735)		(1755)		(1750)		(1760)		(1745)		(1745)		(1715)	
	Δg	$\bar{x}$	−2.81	0.55	1.68	0.60	3.56	1.43	5.56	0.11	10.32	0.78	15.74	0.22	8.34	0.83
	(mgal)	σ	2.76	4.94	7.70	7.54	17.17	6.33	34.73	7.80	36.09	8.50	24.45	6.06	17.21	7.97
	ζ	$\bar{x}$	−0.09	−0.01	0.37	0.02	0.56	0.01	0.59	−0.07	1.90	−0.12	1.30	−0.27	0.38	−0.50
	(m)	σ	0.16	0.13	0.45	0.20	0.78	0.16	1.79	0.19	2.11	0.21	1.42	0.18	1.22	0.26
−46°5			(1730)		(1750)		(1780)		(1780)		(1800)		(1770)		(1745)	
	Δg	$\bar{x}$	4.36	0.76	5.59	−0.11	4.78	−1.50	−9.31	−0.18	14.70	0.18	11.19	1.93	11.75	−0.11
	(mgal)	σ	16.52	4.89	31.50	8.89	54.54	13.09	62.89	10.14	33.07	7.59	13.87	8.05	10.32	8.56
	ζ	$\bar{x}$	0.34	−0.19	0.72	−0.20	0.27	−0.27	−0.92	−0.27	0.55	−0.77	0.66	−0.47	0.66	−0.76
	(m)	σ	0.70	0.12	1.37	0.23	2.72	0.31	3.49	0.25	2.41	0.16	1.34	0.21	0.68	0.25
−45°			(1730)		(1745)		(1780)		(1760)		(1715)		(1740)		(1730)	
	Δg	$\bar{x}$	−0.69	0.43	17.36	0.29	−9.75	−1.63	−26.24	−1.58	−24.64	0.68	−20.19	1.13	2.98	−2.20
	(mgal)	σ	18.63	5.11	31.83	5.17	47.60	10.30	46.96	10.14	33.29	7.93	18.40	6.74	20.99	9.94
	ζ	$\bar{x}$	−0.50	−0.37	0.53	−0.37	−1.18	−0.44	−2.60	−0.47	−2.53	−0.50	−2.51	−0.62	−0.84	−0.96
	(m)	σ	1.06	0.15	1.63	0.13	2.34	0.24	2.35	0.26	1.72	0.20	1.19	0.19	1.47	0.30
−43°5			(1635)		(1670)		(1725)		(1695)		(1660)		(1675)		(1705)	
	Δg	$\bar{x}$	−11.59	0.61	−16.37	−0.47	−0.18	−0.83	17.96	0.20	25.86	0.10	−12.81	1.47	−17.40	−1.57
	(mgal)	σ	6.34	4.55	13.33	4.67	11.71	5.49	14.43	8.01	15.35	10.75	32.01	7.68	19.27	10.24
	ζ	$\bar{x}$	−1.71	−0.42	−2.18	−0.45	−1.85	−0.48	0.67	−0.48	1.04	−0.53	−1.84	−0.62	−2.50	−0.92
	(m)	σ	0.43	0.13	0.79	0.14	0.78	0.14	0.90	0.21	1.12	0.28	1.95	0.18	1.05	0.30
−42°																

Table 5

Prediction of T_{zx}, T_{zy}, $2T_{xy}$ and $T_{yy} - T_{xx}$ from T_{zz} at satellite height (202660 m). Number of input points : 1869 (input area : $40° \leq \varphi \leq 50°$, $1° \leq \lambda \leq 19°$). Number of prediction points : 1344 (prediction area : $41° \leq \varphi \leq 49°$, $2° \leq \lambda \leq 18°$).

Type		obs. (E.U.)	pred. (E.U.)	diff. (E.U.)
T_{zx}	mean	0.01	– 0.01	0.02
	std. dev.	0.14	0.14	0.02
T_{zy}	mean	– 0.01	0.00	– 0.01
	std. dev.	0.08	0.08	0.02
$2T_{xy}$	mean	– 0.04	– 0.01	– 0.03
	std. dev.	0.11	0.11	0.03
$T_{yy} - T_{xx}$	mean	0.00	0.00	0.00
	std. dev.	0.10	0.11	0.03

5. Computation of gravity and geoid heights using FFT

Using the collocation solutions produced as described in section 4, gridded T_{zz} values were computed in the points of a regular $15' \times 20'$ grid at h = 202 and 162 km respectively.

Using FFT as described in Tscherning et al. (1989), values were computed at 5 km height in an identical grid. A first try gave completely wrong results, because no damping of the higher frequencies were made. Using a filter based on the noise and signal variance at 5 km height, new results were obtained, which looked reasonable. Values in a $0°.53 \times 0°.5$ grid, were obtained by interpolation which were compared to the test values. Results with a standard deviation of the differences of 8.0 mgal were obtained.

In order to study the influence of the filter, we varied the supposed noise of T_{zz}. *Figure 13* shows the result as a function of the noise. A relatively broad minimum is found, fortunately close to the actual simulated noise of 0.01 E.U.

6. Evaluation of the simulation results

The area we have investigated is a kind of "worst case" area. The expected gravity anomaly variance of 1400 $mgal^2$ is large considering the extent of the area. Larger variances are generally only found close to trenches.

In this worst case area, we have estimated the error of $0°.5$ mean gravity

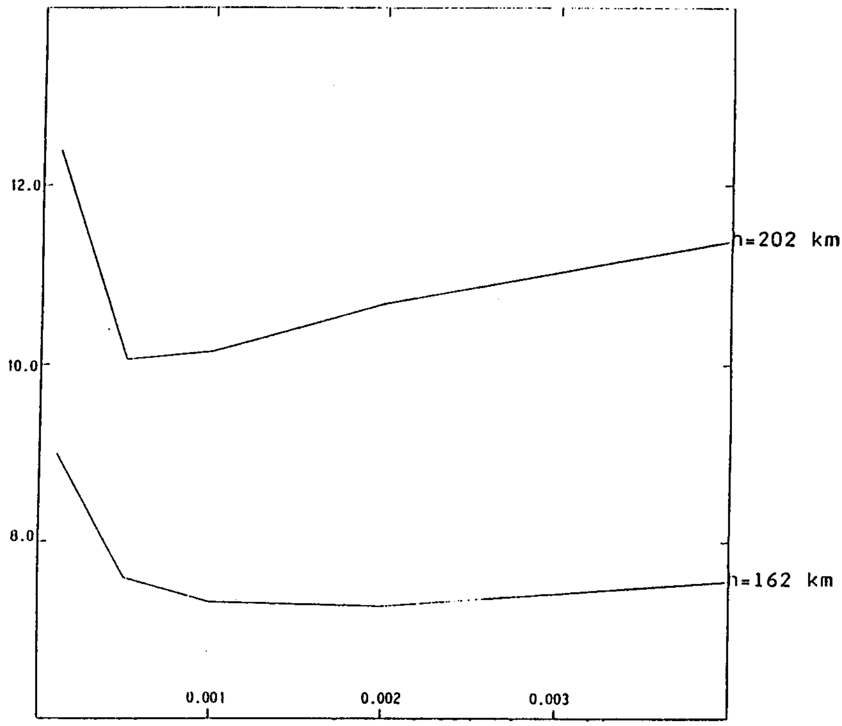

Fig. 13 – Standard deviation of observed minus predicted gravity anomalies at 5 km *altitude using gridded* T_{zz} *values at* h = 202 *and* 162 km *altitude as a function of the observation noise; variance in units of* $(E.U.)^2$.

anomalies to be 7.6 mgal in the best case, disregarding frequencies above degree 360, and 17.0 mgal if we take higher frequencies into account. These results are a factor 2 higher than the results found in Tscherning (1988, *Table 2*). However, there a gravity anomaly variance at the Earth's surface of 400 $mgal^2$ was found, i.e. in terms of standard deviations again factor 2. Our results are therefore consistent with earlier results.

Naturally, the results can be improved. A better reference field will reduce the signal variance, and so will a removal of high-frequency topographic effects. It is realistic to expect the "residual" gravity variance to be between 400 $mgal^2$ and 600 $mgal^2$ for areas as large as the one considered here. In future simulations this should be taken into account.

Besides the simulation results presented here, the investigation has given us other important information :

(a) local solutions may be computed with good results especially in terms of gravity anomalies.

(b) the FFT method works with only a slight degradation of the result.

(c) instrument biases and tilts may be recovered if they are linear for a period up to 40 s (10° orbit piece).

(d) the inclusion of data at the Earth's surface is possible, but does not give an important contribution if the SGG data distribution is good.

(e) the use of several SGG components will only improve slightly the results if T_{zz} data are available. For a combination of other components, the improvement is more substantial.

(f) the GRAVSOFT-package is a flexible tool to carry out simulations as well as actual (regional) gravity field recovery.

Acknowledgement

Thanks to R Forsberg for providing changes to the program GEOFOUR, used to produce the FFT results. This is an abbreviated version of a report to the ESA – CIGAR project, Phase II .

o

o o

REFERENCES

O.L. COLOMBO : The global mapping of gravity with two satellites. *Netherlands Geodetic Commission,* Vol. 7, No. 3, Delft, 1984.

P. KNUDSEN : Estimation and modelling of the local empirical covariance function using gravity and satellite altimeter data. *Bull. Géod., 61,* pp. 145–160, 1987.

W.H. PRESS, B.P. FLANERRY, S.A. TENKOLSKY and W.T. VETTERLING : Numerical recipes. The Art of Scientific Computing. *Cambridge University Press,* Cambridge etc., 1986.

R.H. RAPP and J.Y. CRUZ : Spherical harmonic expansions of the Earth's gravitational potential to degree 360 using 30′ anomalies. *Rep. 376.* Dep. of Geod. Sci. and Surv., The Ohio State University, Columbus, Ohio, 1986.

J.W. ROBBINS : Least squares collocation applied to local gravimetric solutions from satellite gradiometry data. *Rep. 368,* Dep. of Geod. Sci. and Surv. The Ohio State University. Columbus, Ohio, 1985.

C.C. TSCHERNING : A FORTRAN IV program for the determination of the anomalous potential using stepwise least squares collocation. *Rep. 212,* Dep. of Geod. Sci., The Ohio State Univ., Columbus, Ohio, 1974.

C.C. TSCHERNING : Application of collocation for the planning of gravity surveys. *Bull. Géod. 116,* pp. 183–198, 1975.

C.C. TSCHERNING : The role and computation of gravity for the processing of levelling data. *Proceedings Sec. Int. Symposium on Problems Related to the Redefinition of North American Vertical Geodetic Networks,* Ottawa, Canada. May 26-30, 1980, pp. 505–524, Canadian Institute of Surveying, 1980.

C.C. TSCHERNING : Effects of the lack of adequate height and gravity data on the use of positions determined by space techniques in developing countries. *Proceedings of the International Association of Geodesy (IAG) Symposia, Vol. 2,* pp. 658–670, 1983.

C.C. TSCHERNING : A local study of the influence of sampling rate, number of observed components and instrument noise on 1 deg. mean geoid and gravity anomalies determined from satellite gravity gradiometer measurements. Prepared for Dornier System GmbH, Oct. 1987.

C.C. TSCHERNING : A study of satellite altitude influence on the sensitivity of gravity gradiometer measurements. *DGK, Reihe B, Heft Nr. 287* (Festschrift R. Sigl), pp. 218–223, München 1988.

C.C. TSCHERNING : GEOCOL – A FORTRAN program for gravity field approximation by collocation. Technical Note, Geophysical Institute, University of Copenhagen, 9. ed., 1989.

C.C. TSCHERNING, R.H. RAPP and C.C. GOAD : A comparison of methods for computing gravimetric quantities from high degree spherical harmonic expansions. *Manuscripta Geodaetica, Vol. 8*, pp. 249–272, 1983.

C.C. TSCHERNING, R. FORSBERG and M. VERMEER : Methods for regional gravity field modelling from SST and SGG data. Contribution to ESA–CIGAR study, July, 1989.

C.C. TSCHERNING and R.H. RAPP : Closed covariance expressions for gravity anomalies, geoid undulations, and deflections of the vertical implied by anomaly degree-variance models. *Rep. 208*, Dep. of Geod. Sci., The Ohio State University, Columbus, Ohio, 1974.

M. VERMEER : FGI studies on satellite gravity gradiometry. 1st Experiments with a 5–degree buried masses representation. *Report 89:3*, Finnish Geodetic Institute, Helsinki, 1989.

H.-G. WENZEL : Hochauflösende Kugelfunktionsmodelle für das Gravitationspotential der Erde. *Wiss. Arb. Fachrichtung Vermessungswesen der Universität Hannover, Nr. 137*, 1985.

Received : 02.04.1990
Accepted : 05.06.1990